Hindawi Publishing Corporation
Journal of Biomedicine and Biotechnology
Volume 2007, Article ID 26796, 9 pages
doi:10.1155/2007/26796

Research Article

Gel Electrophoresis of Gold-DNA Nanoconjugates

T. Pellegrino,[1,2,3] R. A. Sperling,[1,4] A. P. Alivisatos,[2] and W. J. Parak[1,2,4]

[1] *Center for Nanoscience, Ludwig Maximilians University Munich, 80799 München, Germany*
[2] *Department of Chemistry and Lawrence Berkeley National Lab, University of California, Berkeley, CA 94720, USA*
[3] *National Nanotechnology Laboratory, INFM, 73100 Lecce, Italy*
[4] *Fachbereich Physik, Philipps Universität Marburg, 35037 Marburg, Germany*

Correspondence should be addressed to W. J. Parak, Wolfgang.parak@physik.uni-marburg.de

Received 20 July 2007; Accepted 13 December 2007

Recommended by Marek Osinski

Gold-DNA conjugates were investigated in detail by a comprehensive gel electrophoresis study based on 1200 gels. A controlled number of single-stranded DNA of different length was attached specifically via thiol-Au bonds to phosphine-stabilized colloidal gold nanoparticles. Alternatively, the surface of the gold particles was saturated with single stranded DNA of different length either specifically via thiol-Au bonds or by nonspecific adsorption. From the experimentally determined electrophoretic mobilities, estimates for the effective diameters of the gold-DNA conjugates were derived by applying two different data treatment approaches. The first method is based on making a calibration curve for the relation between effective diameters and mobilities with gold nanoparticles of known diameter. The second method is based on Ferguson analysis which uses gold nanoparticles of known diameter as reference database. Our study shows that effective diameters derived from gel electrophoresis measurements are affected with a high error bar as the determined values strongly depend on the method of evaluation, though relative changes in size upon binding of molecules can be detected with high precision. Furthermore, in this study, the specific attachment of DNA via gold-thiol bonds to Au nanoparticles is compared to nonspecific adsorption of DNA. Also, the maximum number of DNA molecules that can be bound per particle was determined.

1. INTRODUCTION

DNA-functionalized gold nanoparticles are an interesting system with applications ranging from biological sensors to the construction of self-assembled materials. Experiments are based on attaching single-stranded DNA molecules via thiol-gold bonds to the surface of Au nanoparticles and a subsequent self-assembly process of these conjugates by making use of base pairing of complementary DNA molecules [1–5]. For example, by employing Au-DNA conjugates, several groups have developed schemes to detect target DNA sequences [6] and to assemble nanoparticles into macroscopic materials [7, 8]. DNA-functionalized Au nanoparticles are the building blocks for the above-mentioned experiments. Therefore, it is of great interest to investigate the properties of these conjugates in detail.

Due to the high affinity of thiol groups to gold surfaces, thiol-modified DNA molecules can be directly bound to the surface of citrate- or phosphine-stabilized Au nanoparticles [9, 10]. Although commonly a random number of DNA molecules are attached per Au nanoparticle [1], also particles with an exactly defined number of one, two, or three attached DNA molecules per nanoparticles can be obtained [11–15]. Certainly, several parameters have significant influence on the properties of Au-DNA conjugates, such as coverage of the Au surface with DNA, configuration of the attached DNA molecules, and hybridization efficiency of DNA attached to Au surfaces. These parameters are strongly connected. The degree of DNA coverage will influence the DNA conformation, which, in turn, will affect the hybridization efficiency. Also, nonspecific adsorption has to be considered.

A body of experiments investigating these parameters has been reported for DNA attached to flat Au surfaces using different techniques such as atomic force microscopy (AFM) [16–18], surface plasmon resonance (SPR) spectroscopy [19–21], radioisotopic techniques [22, 23], ellipsometry [23], and X-ray photoelectron spectroscopy (XPS) [23]. These experiments allow for a detailed picture of DNA bound to planar gold surfaces and the results have clarified

T. Pellegrino and R. Sperling contributed equally to the work.

the binding mechanism, the surface coverage, the hybridization efficiency, and the role of nonspecific adsorption, all in dependence of the length of the DNA.

Since the effect of surface curvature has to be taken into account [24], the results obtained for planar Au surfaces may be transferred to spherical Au nanoparticles only under certain restrictions. The surface coverage of Au nanoparticles with DNA has been investigated using the displacement of fluorescence-labeled DNA molecules with mercaptoethanol [25] and by gel electrophoresis [26]. Also, the conformation of bound DNA [27, 28], hybridization [29], and the role of nonspecific adsorption [26, 28, 30] have been investigated for Au nanoparticles.

In this report, we present a detailed study of electrophoretic mobility of Au-DNA conjugates. With this study, we want to determine the possibilities and limitations of this technique. Besides our own previous work [27, 31], also other groups [28, 32, 33] have recently reported about the possibility to extract effective diameters for bioconjugated colloidal nanoparticles from electrophoretic mobilities. The aim of this study is, in particular, to investigate the limitations of this analysis.

2. MATERIALS AND METHODS

2.1. Sample preparation

Citrate-coated gold nanoparticles of 5, 10, and 20 nm diameter were purchased from BBI/TED Pella (Redding, Calif, USA). In order to improve their stability in buffer solution, the adsorbed citrate molecules were replaced by a phosphine (bis(p-sulfonatophenil)phenylphosphine dehydrate, dipotassium salt) [11]. The concentration of the Au nanoparticles was determined by UV/vis spectroscopy by using the molecular extinction coefficient of their absorption at the plasmon peak. Thiol- and Cy5-modified and unmodified single-stranded DNA were purchased from IDT (Coralville, Iowa, USA) or Metabion (München, Germany). All sequences can be found in the Supplementary Material (available online at doi: 10.1155/2007/ 26796). The concentration of the DNA was determined by UV/vis spectroscopy by using the molecular extinctions coefficient of their absorption at 260 nm. The thiol-modified and plain DNA were added to the phosphine-coated Au nanoparticles at pH = 7.3, c (NaCl) = 50 mM, and samples were incubated for some hours up to several days [11, 27]. Generally, in such experiments, DNA is always added in large excess, thus that the number of attached molecules is related but not fully controlled by the stoichiometry of DNA:Au-NP because of the rather low binding yield.

2.2. Gel electrophoresis experiments

The resulting Au-DNA conjugates were loaded on 0.5%–6% agarose gels (agarose: Gibco BRL, number 15510-027; 0.5 × TBE buffer, pH 9) and run for one hour at 100 V [11, 27]. (Since 6% gels can be inhomogeneous due to their high viscosity, the data obtained with these gels have to be interpreted with care.) As reference, always unconjugated Au nanoparticles of the same diameter were run on the same gel. In addition, gels with unconjugated Au nanoparticles of different diameter and free DNA of different length were run. The bands of the plain and DNA-conjugated Au nanoparticles were directly visible by the red color of the Au colloid and the free DNA was visualized by an attached fluorescence label (fluorescein, Cy3, or Cy5). The bands of the gels were photographed using a digital camera system (Eagle Eye III, Stratagene). The mobility of each sample was determined by measuring the position of each band referring to the start position where the samples had been loaded. This resulted in a comprehensive set of data which relates the mobility of Au-DNA conjugates to the diameter of the Au particles, where the relation between the amount and the length of the attached DNA, nonspecific versus specific attachment via thiol-gold bonds, and the gel percentage was studied.

2.3. Calculation of the effective diameter of the Au-DNA conjugates

Since mobility is not an illustrative quantity, we have attempted to convert the mobilities of Au-DNA conjugates in effective diameters. The evaluation of the gels in which plain Au-nanoparticles of known diameter were run yielded a calibration curve in which the mobility is plotted versus the diameter. By using this calibration curve, the mobility of the Au-DNA conjugates could be directly converted into effective diameters [27]. Alternatively, the mobility of Au-DNA conjugates at different agarose concentrations was used to obtain Ferguson plots [34] and fits of the Ferguson plots yielded the retardation coefficients [28]. First, Ferguson plots were made for plain Au-nanoparticles of known diameter and a calibration curve in which the retardation coefficients were plotted versus the particle diameter was obtained [28]. By using this calibration curve, the effective diameters of Au-DNA conjugates could be derived from the retardation coefficients derived from the Ferguson plots of the Au-DNA conjugates [28].

2.4. Determination of the maximum number of attached DNA molecules per particle

We have also quantified the maximum number of DNA molecules that can be attached per gold nanoparticle for particles with 5 nm and 10 nm diameter and single-stranded DNA with 8 and 43 bases. For this purpose, single-stranded DNA that had been modified with a thiol group on the 3' and a Cy5 dye on the 5' end has been attached via formation of thiol-Au bonds to the surface of Au particles. DNA was added in different DNA to Au ratios and the conjugates were run on an agarose gel. The more DNA bound per Au nanoparticle, the more the band of this conjugate was retarded on the gel [27]. At a certain amount of added DNA, the retardation of the band of the conjugates did not further increase, which indicates that the Au surface is fully saturated with DNA [27]. The bands were extracted from the gel by cutting out the agarose piece that contained the band and immersing it into 0.5 × TBE buffer solution. After two days, the Au-DNA conjugates had diffused out of the gel into the buffer. The

extraction procedure ensures that all DNA is really attached to the Au particles, since free DNA migrates in a much faster band. UV/vis spectra were recorded of the extracted Au-DNA conjugates. For each of the conjugates, the DNA concentration was determined by the Cy5 absorption and the Au concentration was determined by the absorption at the plasmon peak and from both concentrations the number of attached DNA molecules per particles was derived. As we quantified the number of attached Cy5 molecules only with absorption and not with fluorescence measurements, the effect that the fluorescence of Cy5 close to Au surfaces is quenched [35] did not interfere with our analysis.

All methods and additional experiments can be found in detail in the supplementary material.

3. RESULTS AND DISCUSSION

3.1. The attachment of DNA to particles increases the effective diameter and thus lowers the electrophoretic mobility

The attachment of DNA to Au nanoparticles can be clearly observed by gel electrophoresis [9, 11, 13, 26–28, 36–38]. The mobility of particles on the gel depends on two factors: size and charge. The bigger the size, the slower and the higher the charge, the faster particles will migrate. In the case of negatively charged Au particles (e.g., with citrate or phosphine molecules adsorbed to the particles), the attachment of negatively charged DNA molecules causes in first place an increase of size that can be seen as a retardation of the band of the gel [27]. If the change in charge dominated, then the mobility of the Au particles should be increased (addition of negative charge) or drastically decreased (addition of positive charge) up to change in the direction of migration. Although this effect has been observed for different systems [31, 39], it has not been observed for the Au-DNA conjugates used in this study. Upon attachment of DNA, the mobility of the resulting conjugates was always moderately decreased. Therefore, in agreement with previous reports, we assume throughout this manuscript that attachment of DNA to Au nanoparticles in first order increases the effective diameter of the conjugates which can be directly seen in the retardation of the band of the conjugates in gel electrophoresis experiments [9, 11, 26–28, 36–38].

3.2. Generation of a calibration curve that relates electrophoretic mobilities to effective diameters

One aim of this study was to obtain calibration curves in which measured electrophoretic mobilities m can be related to effective diameters d_{eff}. By running phosphine-stabilized Au particles of known diameter (the overall diameter of phosphine-coated Au NP was assumed as the core diameter plus two times 0.5 nm for the thickness of the phosphine layer and the smallest nanoparticle size used for calibration was 6 nm) on gels, by measuring their mobility, by fitting the data empirically with an exponential function, and by using the inverse of the fit function, we obtained a function in which the effective diameter of Au particles and Au-DNA conjugates can be directly calculated from their electrophoretic mobility:

$$d_{\text{eff}}(m) = -T_y * \ln((m/m_{10\,\text{nm},y})/A_y) + 6\,\text{nm}. \quad (1)$$

Table 1: Experimentally obtained parameters for deriving effective diameters from electrophoretic mobilities for different gel percentages y. The data have been derived by fitting an experimentally obtained dataset of electrophoretic mobilities of Au nanoparticles of known diameter and represent the mean values and standard deviations.

y	A_y	T_y (nm)
0.5%	1.017 ± 0.015	189 ± 19
1%	1.049 ± 0.012	85.0 ± 3.7
2%	1.120 ± 0.024	37.7 ± 1.9
3%	1.236 ± 0.025	18.8 ± 0.8
4%	1.476 ± 0.061	10.3 ± 0.9
5%	1.759 ± 0.079	7.16 ± 0.66
6%	2.073 ± 0.083	5.77 ± 0.49

The parameters for y = 0.5%, 1%, 2%, 3%, 4%, 5%, and 6% agarose gels are enlisted in Table 1. In order to enhance the accuracy by making relative instead of absolute measurements, we always normalized the mobilities m to the mobilities $m_{10\,\text{nm},y}$ of plain phosphine-stabilized Au particles of 10 nm core diameter on the same gel. Therefore, although the primary data of all electrophoresis measurements are electrophoretic mobilities, we are discussing the experimental results in terms of effective diameters. The diameters have been obtained with the above-described formula from the mobility data.

Since obviously the effective diameter of Au-DNA conjugates is a fixed physical property, it should not depend on the form of measurement and analysis. We, therefore, compared the effective diameters derived from 1%, 2%, 3% gels via the respective mobility-diameter calibration curves and from Ferguson plots [34]. For the Ferguson plots, the mobility data from all gel percentages are required.

3.3. Evaluation of the accuracy of effective diameters obtained from electrophoretic mobilities via mobility-diameter calibration curves

The determined effective diameters for Au-DNA conjugates for Au particles saturated with DNA and for Au particles with only few DNA strands attached per particle are plotted in Figures 1 and 2 for DNA of different length. In all cases, regardless the length of the DNA, whether DNA was attached by specific thiol-gold linkage or by nonspecific adsorption, or whether only a few or a many as possible DNA molecules were bound per Au nanoparticles, the effective diameters derived with the mobility-diameter calibration curves are different for different gel percentages. Though most of the times the effective diameters derived from gels with higher percentage were found to be larger than the ones obtained from gels with lower percentage, also the opposite effect was observed within the experimental error bars (see, e.g., Figure 2). The

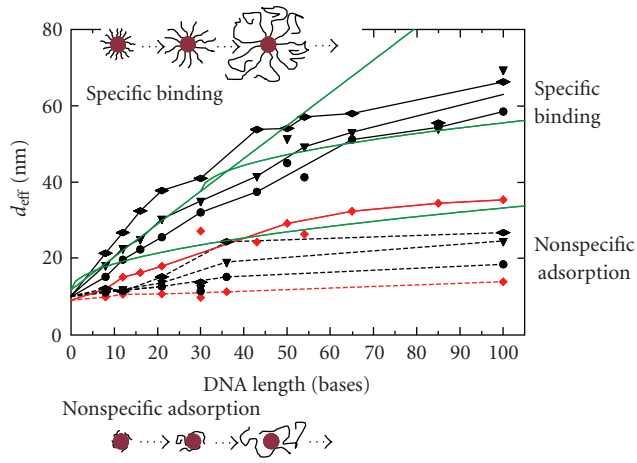

Figure 1: Effective diameter d_{eff} of Au-DNA conjugates for Au surfaces saturated with DNA. The surface of 10 nm phosphine-stabilized Au nanoparticles was saturated with single-stranded DNA of different lengths and the conjugates were run on 1%, 2%, and 3% gels. From the measured mobilities, the effective diameters of the conjugates were determined. The effective diameters obtained from 1%, 2%, and 3% gels are plotted in black with diamond, triangle, and circle symbols, the effective diameters obtained from Ferguson analysis are plotted in red. The effective diameters of conjugates in which the DNA was linked to the Au particles via specific thiol-gold bonds are connected with straight lines, the effective diameters of conjugates in which the DNA is nonspecifically adsorbed to the Au particles are connected with dotted lines. The green lines correspond to rudimentary theoretical models of the effective diameters of DNA molecules attached via thiol-gold to Au particles [27]. For fully stretched DNA (bottom curve), $d_{\text{eff, linear}}(N) = 10\,\text{nm} + 2\,.\,(0.92\,\text{nm} + N.\,0.43\,\text{nm})$, for randomly coiled DNA (top curve) $d_{\text{eff, coil}}(N) = 10\,\text{nm} + 2\,.\,(0.92\,\text{nm} + 2\,.\,[3^{-1}.N.\,0.43\,\text{nm}\,.\,2\,\text{nm}]^{1/2})$, and for DNA partly stretched and partly coiled DNA (middle curve) $d_{\text{eff,mixed}}(N) = 10\,\text{nm} + 2\,.\,(0.92\,\text{nm} + 30\,.\,0.43\,\text{nm} + 2\,.\,[3^{-1}.\,(N-30)\,.\,0.43\,\text{nm}\,.\,2\,\text{nm}]^{1/2})$ was used [27]. We assumed 0.92 nm for the length of the thiol-hydrocarbon (C_6) spacer at the reactive end of the DNA, 0.43 nm per base for the contour length and 2 nm for the persistence length [42, 43]. N corresponds to the number of bases.

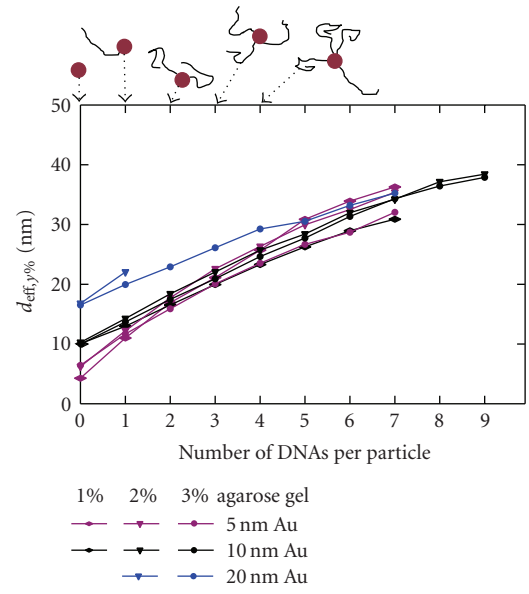

Figure 2: Effective diameter of Au-DNA conjugates with a discrete number of DNA molecules attached per Au nanoparticle. 10 nm Au particles were incubated with thiol-modified single-stranded DNA of 43 and 100 bases length and run on 1%, 2%, and 3% agarose gels. On the gels, particles with exactly $0, 1, 3, 4, \ldots$ DNA molecules attached per Au particle could be identified as discrete bands. From the mobilities of the bands on the gels, the effective diameters d_{eff} were derived by using a calibration curve that relates mobilities and diameters. The effective diameters corresponding to effective diameters derived from 1%, 2%, and 3% gels are plotted in black with diamond, triangle, and circle symbols, respectively. From the mobility data of the gels of different percentage effective diameters were also obtained by the Ferguson method and are plotted in red. The upper and lower sets of curves belong to the Au-DNA conjugates with 100 bases and 43 bases DNA, respectively.

effective diameters derived from Ferguson plots were always smaller than the ones derived from the mobility-diameter calibration curves. This clearly demonstrates a severe limitation of deriving effective diameters from electrophoretic mobilities. If always the effective diameters derived from the gels of higher percentage were smaller than the one derived from gels with lower percentage, one could have argued that the soft DNA shell around the rigid Au cores would be squeezed or compressed more while migrating through the gel of higher agarose concentration, which would lead to smaller effective diameters. However, since no clear correlation between the gel concentration and the derived effective diameters was observed, we have to consider the difference between the effective diameters that have been obtained from gels of different concentrations as error bars. The bigger the Au particles become due to attachment of DNA, the bigger the error in deriving their effective diameter from electrophoretic mobilities becomes. For example, according to Figure 1, the effective diameters of 10 nm Au particles saturated with 100 bases DNA that is specifically linked via thiol-Au bonds are 66.3 nm, 69.5 nm, and 58.5 nm as determined from 1%, 2%, and 3% gels. We believe that from these data we can assume that the effective diameter of these conjugates is around 60 nm with an error bar of around 10 nm. From these and additional similar data (not shown), we conclude that deriving absolute effective diameters from electrophoretic mobilities via mobility-diameter calibration curves is possible only under certain restrictions. It is not sufficient to extract the data just from gels of one percentage. Only by using gels of different percentage an average value for the effective diameter and an estimate about the error can be obtained. Part of this limitation might be due to our principal assumption that in the case of phosphine-stabilized Au particles conjugated with DNA, the electrophoretic mobility is in first order only determined by the size of the conjugates. Charge effects may hamper obtaining more precise data for effective diameters. For other systems in which charge effects certainly will play a more important role [39], it might be even impossible to derive effective diameters from electrophoretic mobilities with the here-reported mobility-diameter calibration curves. It also has to be pointed out that the possible application of

the here-reported calibration curves is limited to relatively rigid objects similar in nature to Au nanoparticles. As these objects were used in first order to obtain the experimental data on which the calibration functions are based, the calibration functions certainly will not describe the diameters of soft objects, such as DNA, very well. A likely explanation for the deviation in the effective diameters obtained for the DNA-Au conjugates with the calibration functions for the gels of different percentage can be seen in the fact that the calibration functions are directly only applicable for Au particle-like rigid objects. Attaching soft objects as DNA to the Au particle surface changes their electrophoretic behavior so that the calibration curves can be only applied in a restricted way.

3.4. Evaluation of the accuracy of effective diameters obtained from Ferguson plots

We have also evaluated the possibility to obtain effective diameters of Au-DNA conjugates via Ferguson plots, as had already suggested by the group of Hamad-Schifferli [28]. From Figures 1 and 2, it is evident that the effective diameters obtained from Ferguson plots are always significantly smaller than the ones obtained from mobility-diameter calibration curves. It has to be pointed out that both evaluation methods are based on the same set of experimentally obtained mobilities. In a classical Ferguson plot, for example for free DNA, the logarithm of the mobilities is linear to the gel percentage. However, in the case of Au and Au-DNA conjugates, this linearity holds no longer true, in particular for gels of higher percentage [36]. We, therefore, had to restrict our analysis to gels from 1% to 3% although in some cases data for 4% to 6% had also been available. Additional experiments can be found in the supplementary material. Though theories for nonlinear, convex Ferguson plots exist [40, 41], we did not try to apply them here. Due to the significant deviation from the data obtained with the Ferguson plots to the data obtained with mobility-diameter calibration curves and due to the above-mentioned limitations, we conclude that the linear Ferguson analysis is less suited to obtain absolute effective diameters. However, relative increases in size due to binding of molecules can be observed with sufficient resolution with Ferguson analysis.

3.5. Specific thiol-Au bond-mediated attachment of DNA versus nonspecific DNA adsorption

Our data clearly indicate that there is also nonspecific adsorption of DNA to the surface of Au particles in case the particles are exposed to many DNA molecules, see Figure 1. It is important to point out that in Figure 1, the data of Au particles that have been exposed to as much DNA as possible and that are, therefore, saturated with DNA are described. This is different from the case in which the Au particles are exposed to only to a few strands of DNA as in Figure 2, where no nonspecific adsorption could be observed, as already reported by Zanchet et al. [11]. Nonspecific adsorption of DNA to Au particles is significantly lower compared to specific thiol-Au bond-mediated attachment and thus can only be observed in case of exposure of the particles to very high DNA concentrations.

Although the absolute numbers derived for effective diameters for Au-DNA conjugates are afflicted with significant error bars as described above, these data nevertheless contain valuable information about the binding of DNA to Au particles. Any attachment of DNA leads to an increase in the effective diameter, dependent on the nature of attachment, the amount of bound DNA, and the length of each DNA molecule, see Figure 1. With very simple models, we can assume that DNA attached to the surface of Au particles can adopt two basic types of conformation [27]. In the first case, the confirmation of DNA is not effected by the presence of the Au particles and it will form a random coil. In the second case, DNA has to compete for the binding places at the gold surface and thus, in order to bind as many DNA molecules per area as possible, the DNA has to be stretched. Actually, a combination of both models will best describe the reality. In Figure 1, the effective diameters for the different models (randomly coiled DNA, fully stretched DNA, and DNA that is stretched for the first 30 bases and randomly coiled for the rest of the bases) are plotted versus the DNA length for Au particles that are saturated with DNA. Clearly, thiol-gold-bond specific attachment can be distinguished from nonspecific adsorption of DNA. Similar observations have been reported also before by Sandström et al. [26, 37]. First, the increase in the effective diameter tells that also DNA without thiol modification can be adsorbed to the surface of phosphine-stabilized Au nanoparticles. Second, a comparison with the effective diameters of the theoretical models clearly proves that nonspecifically adsorbed DNA does not exist in a stretched configuration perpendicular to the Au surface. The data rather indicate that even when the particle surface is saturated with nonspecifically attached DNA, only parts of the DNA molecules will be randomly coiled, as the experimentally obtained effective diameters are smaller than the diameter of conjugates in which the adsorbed DNA is randomly coiled. From this, one can conclude that due to nonspecific Au-DNA interaction, the adsorbed DNA is at least partly wrapped around the surface of the Au particles, which is in agreement with other studies [44]. In case of Au surfaces saturated with thiol-modified DNA, the effective diameters are significantly bigger compared to nonspecifically adsorbed DNA, see Figure 1. By comparison with basic models, we conclude in agreement to our previous study that specifically bound DNA adopts a stretched configuration so that as many DNA molecules as possible can bind to the Au surface. Due to the spherical geometry, DNA longer than around 30 bases only needs to be stretched due to this space limitation within around the first 30 bases, whereas the parts of the DNA molecules further away from the Au particle are not affected by space limitation and thus can be randomly coiled. These results again show the possibilities and limitations of the here-described method. Though it is complicated to derive accurate absolute effective diameters of Au-DNA conjugates, the binding of DNA molecules can be clearly seen as an increase in the effective diameters and a comparison with theoretical models can give indications about the conformation of the attached DNA. These

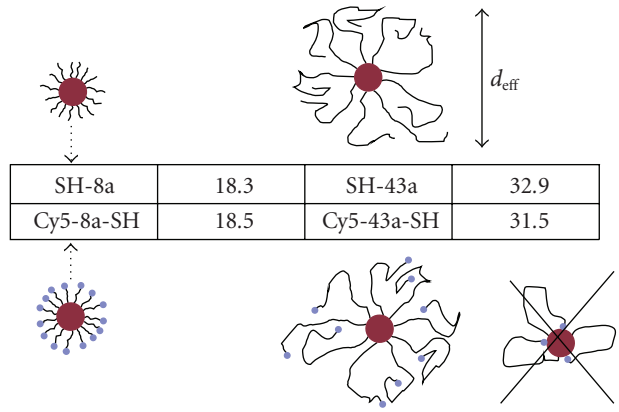

SH-8a	18.3	SH-43a	32.9
Cy5-8a-SH	18.5	Cy5-43a-SH	31.5

Figure 3: 10 nm diameter Au particles have been saturated with thiol-modified single-stranded DNA of 8 and 43 bases lengths and were run on 2% agarose gels. From the resulting mobilities, effective diameters were derived via a mobility-diameter calibration curve (for 2% agarose gels). In the table, the effective diameters of particles are given in nm. In the upper row, the data for DNA modified at one end with an-SH group are shown. In the bottom row, the data for DNA modified at one end with an-SH and at the other end with a -Cy5 organic fluorophore are shown. The results are within the error bars identical for DNA with and without Cy5, which indicates that the Cy5 at the free end does not interfere with the binding process of the DNA to the Au particle surface.

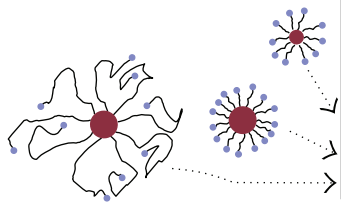

d(Au) (nm)	Number of bases per DNA	Maximum number of DNA molecules per Au particle	Maximum DNA density on the particle surface (nm^{-2})
5	8	13	0.041
10	8	53	0.042
10	43	43	0.033

Figure 4: Maximum number of thiol-modified single-stranded DNA molecules that can be bound to the surface of phosphine-stabilized Au particles. Au particles of different core-diameter (d = 5 nm, 10 nm) and thiol modified single-stranded DNA of different length (8 and 43 bases) have been used. The maximum possible number of DNA molecules per Au particle and the maximum surface density (in DNA per particle surface) are given.

types of binding assays via gel electrophoresis are an attractive complementary method compared to other techniques, such as light scattering [45]. Presumably a combination of gel electrophoresis, light scattering, and zeta potential measurements of identical samples would give the most accurate analysis about Au-DNA conjugates. It remains to note that although electrophoresis of free DNA is well studied both experimentally and theoretically, the case of Au-DNA conjugates is more complex because several properties (total charge, charge density, and elasticity) are not constant but depend all at the same time on the binding of DNA to the Au nanoparticles. A theoretical model for gel electrophoresis of such conjugates would be helpful for data analysis.

3.6. Effect of organic fluorophores linked to DNA on the binding of DNA to Au particles

When organic fluorophores are attached to Au-DNA conjugates at the free end of the DNA, which is pointing towards solution, then energy transfer between the fluorophore and the Au nanoparticle can be observed [35]. This effect can be, for example, employed for DNA sensors [46]. Since energy transfer depends on the distance between the organic fluorophore and the Au surface [35, 47], certainly the configuration of the bound fluorophore-modified DNA is important for this process. In case of nonspecific adsorption of the fluorophore to the Au surface, the distance between the fluorophore and the Au would be much smaller than for the case in which the DNA is linked with its thiol-modified end, see Figure 3. In this study, we have shown that the attachment of Cy5 to the free end of thiol-modified DNA does not change the effective diameter in the case of Au particles saturated with DNA, see Figure 3. These results demonstrate that the direct adsorption of Cy5 to the Au surface is much less probable than the formation of thiol-Au bonds and that, therefore, the dye points towards the solution.

3.7. Determination of the maximum number of DNA molecules that can be bound per one Au particle

The number of bound DNA molecules per Au particle has already been determined with several methods [25, 26, 48].

In comparison to methods in which the number of DNA molecules is quantified by the fluorescence of attached fluorophores, the counting of DNA via absorption measurements (as reported in this study) is not affected by photobleaching and quenching effects. Extracting the Au-DNA conjugates from the gel also helps that no unbound excess DNA is present in the solution, as it still might be possible in the case of purification with filter membranes. The results of this study are summarized in Figure 4 and are in the same range as the results obtained by other groups [25, 26, 48] though our determined DNA densities are rather lower than the ones determined by other groups. This might be due to the fact that the phosphine stabilization is harder to be displaced by DNA than citrate stabilization and in particular due to the fact that our incubation was performed at lower NaCl concentrations [48]. In our measurements, we could not find any effect of the different curvature between 5 nm and 10 nm gold particles on the density of attached DNA molecules. This can be understood as the surface curvature difference between both types of particles is not very high and DNA attachment to both types of particles was done under the same buffer conditions. Recently, Qin and Yung have instead demonstrated that the most relevant parameter for the maximum number of attached DNA molecules per particle is the salt concentration under which the attachment was performed [48]. High salt concentrations reduce electrostatic repulsion und thus allow for higher DNA surface densities.

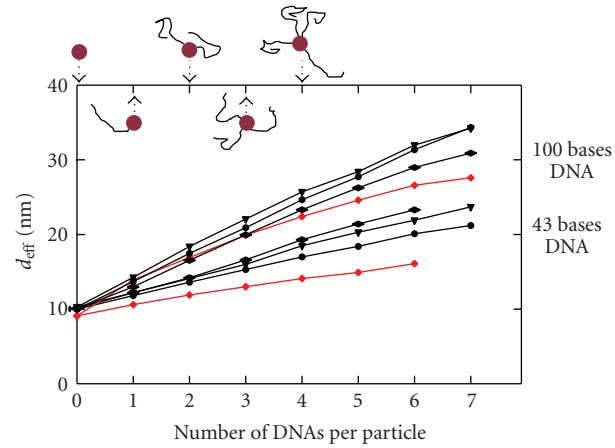

FIGURE 5: Effective diameters d_{eff} of Au-DNA conjugates with a discrete number of DNA molecules per particle for Au particles of different diameter. Single-stranded DNA (100 bases) had been specifically attached via thiol-gold bonds to the surface of 5 nm, 10 nm, and 20 nm Au particles. The conjugates were run on 1%, 2%, and 3% agarose gels and their effective diameters d_{eff} were derived from the measured electrophoretic mobilities. Here, the effective diameters for Au particles with a discrete number of attached DNA molecules (100 bases) per particle are shown. Data for 5 nm, 10 nm, and 20 nm particles are plotted in violet, black, and blue, respectively. Data derived from 1%, 2%, and 3% gels are plotted with diamond, triangle, and circle symbols.

3.8. *Attachment of an exactly known number of DNA molecules per Au particle*

As already reported in earlier publications, gel electrophoresis allows for a separation of Au-DNA conjugates with $0, 1, 2, \ldots$ DNA molecules attached per particle [9, 11]. In Figures 2 and 5, the effective diameters of such conjugates as determined from their electrophoretic mobilities are presented. The dependence of DNA length and Au core diameter on the effective diameter is as expected. The longer the DNA, the more the effective diameter of Au-DNA conjugates upon which attachment of another DNA molecule to one gold particle is increased (see Figure 2). The more long DNA strands are attached per individual gold particle, the fewer the effective diameter of the Au-DNA conjugated depends on the initial diameter of the Au core (see Figure 5). Although no simple model for Au-DNA conjugates is available that could predict the exact mobility in gel electrophoresis, the bands of particles with a defined number of DNA strands can be identified with their structure by relative (qualitative) comparison and control experiments that include hybridization. So far, we are not aware of another separation technique (such as HPLC) that can resolve Au particles with an individual number of attached DNA molecules as it is possible with gel electrophoresis. The concept of separating conjugates of particles with a discrete number of attached molecules by gel electrophoresis could be also be generalized and used besides for Au-DNA conjugates for other systems [49]. Because of their defined composition, we think that such conjugates of particles with a defined number of linked molecules are very interesting model systems and several applications have been already demonstrated [50, 51].

4. CONCLUSIONS

In this manuscript, the analysis of Au-DNA conjugates by gel electrophoresis is discussed. Whereas the principal effects are already known by our previous studies and reported by other groups, the aim of this work was the detailed analysis about the possibilities and limitations of this technique. For this purpose, an extensive study with 1200 gels was performed. From these data, we can conclude that the determination of absolute effective diameters from electrophoretic mobilities has severe limitations. In order to get an estimate about the accuracy of the data gels of different percentages have to be compared. The deviation between these data sets is an indicator for the error bars in the derived effective diameters. We believe that this strategy leads to more reliable values for effective diameters than Ferguson analysis. Pointing out these limitations is important as several studies exist in which this method has been applied without investigating its limitations first [27, 28, 32]. Though the extraction of absolute values for effective diameters from the mobility data has very limited accuracy, the attachment of molecules to particles can on the other hand be detected with high sensitivity as an increase in the effective diameters. In this way, even the attachment of single molecules can be resolved, which to our knowledge has not been demonstrated yet with an alternative separation technique such as HPLC. Besides such binding assays, also

indications about the conformation of the DNA molecules that are bound to the particles can be derived from the obtained effective diameters. In this way, we believe that gel electrophoresis is a very powerful method to investigate the attachment of DNA molecules to Au nanoparticles though it has also clear limitations. Whereas specific and nonspecific attachment of DNA can be detected with high sensitivity, the quantitative determination of effective hydrodynamic diameters is not possible in a straightforward way.

ACKNOWLEDGMENTS

The authors are grateful to Dr. Eric Dulkeith for helpful comments. This work was supported in part by the German Research Foundation (DFG, Emmy Noether program), the European Union (STREP program NANO-SA), the Center for Nanoscience (CeNS), and the U.S. Department of Energy (Contract no. DE-AC02-05CH11231).

REFERENCES

[1] W. Fritzsche and T. A. Taton, "Metal nanoparticles as labels for heterogeneous, chip-based DNA detection," *Nanotechnology*, vol. 14, no. 12, pp. R63–R73, 2003.

[2] C. A. Mirkin, "Programming the assembly of two- and three-dimensional architectures with DNA and nanoscale inorganic building blocks," *Inorganic Chemistry*, vol. 39, no. 11, pp. 2258–2272, 2000.

[3] E. Dujardin and S. Mann, "Bio-inspired materials chemistry," *Advanced Materials*, vol. 14, no. 11, pp. 775–788, 2002.

[4] Z. Wang, R. Lévy, D. G. Fernig, and M. Brust, "The peptide route to multifunctional gold nanoparticles," *Bioconjugate Chemistry*, vol. 16, no. 3, pp. 497–500, 2005.

[5] A. G. Kanaras, Z. Wang, A. D. Bates, R. Cosstick, and M. Brust, "Towards multistep nanostructure synthesis: programmed enzymatic self-assembly of DNA/gold systems," *Angewandte Chemie International Edition*, vol. 42, no. 2, pp. 191–194, 2003.

[6] R. Elghanian, J. J. Storhoff, R. C. Mucic, R. L. Letsinger, and C. A. Mirkin, "Selective colorimetric detection of polynucleotides based on the distance-dependent optical properties of gold nanoparticles," *Science*, vol. 277, no. 5329, pp. 1078–1081, 1997.

[7] C. A. Mirkin, R. L. Letsinger, R. C. Mucic, and J. J. Storhoff, "A DNA-based method for rationally assembling nanoparticles into macroscopic materials," *Nature*, vol. 382, no. 6592, pp. 607–609, 1996.

[8] A. Paul Alivisatos, K. P. Johnsson, X. Peng, et al., "Organization of 'nanocrystal molecules' using DNA," *Nature*, vol. 382, no. 6592, pp. 609–611, 1996.

[9] C. J. Loweth, W. Brett Caldwell, X. G. Peng, A. Paul Alivisatos, and P. G. Schultz, "DNA-based assembly of gold nanocrystals," *Angewandte Chemie International Edition*, vol. 38, no. 12, pp. 1808–1812, 1999.

[10] R. L. Letsinger, R. Elghanian, G. Viswanadham, and C. A. Mirkin, "Use of a steroid cyclic disulfide anchor in constructing gold nanoparticle-oligonucleotide conjugates," *Bioconjugate Chemistry*, vol. 11, no. 2, pp. 289–291, 2000.

[11] D. Zanchet, C. M. Micheel, W. J. Parak, D. Gerion, and A. Paul Alivisatos, "Electrophoretic isolation of discrete Au nanocrystal/DNA conjugates," *Nano Letters*, vol. 1, no. 1, pp. 32–35, 2001.

[12] K.-M. Sung, D. W. Mosley, B. R. Peelle, S. Zhang, and J. M. Jacobson, "Synthesis of monofunctionalized gold nanoparticles by Fmoc solid-phase reactions," *Journal of the American Chemical Society*, vol. 126, no. 16, pp. 5064–5065, 2004.

[13] S. D. Jhaveri, E. E. Foos, D. A. Lowy, E. L. Chang, A. W. Snow, and M. G. Ancona, "Isolation and characterization of trioxyethylene-encapsulated gold nanoclusters functionalized with a single DNA strand," *Nano Letters*, vol. 4, no. 4, pp. 737–740, 2004.

[14] C. J. Ackerson, M. T. Sykes, and R. D. Kornberg, "Defined DNA/nanoparticle conjugates," *Proceedings of the National Academy of Sciences of the United States of America*, vol. 102, no. 38, pp. 13383–13385, 2005.

[15] W. J. Qin and L. Y. L. Yung, "Nanoparticle-DNA conjugates bearing a specific number of short DNA strands by enzymatic manipulation of nanoparticle-bound DNA," *Langmuir*, vol. 21, no. 24, pp. 11330–11334, 2005.

[16] N. Mourougou-Candoni, C. Naud, and F. Thibaudau, "Adsorption of thiolated oligonucleotides on gold surfaces: an atomic force microscopy study," *Langmuir*, vol. 19, no. 3, pp. 682–686, 2003.

[17] E. Huang, M. Satjapipat, S. Han, and F. Zhou, "Surface structure and coverage of an oligonucleotide probe tethered onto a gold substrate and its hybridization efficiency for a polynucleotide target," *Langmuir*, vol. 17, no. 4, pp. 1215–1224, 2001.

[18] E. Huang, F. Zhou, and L. Deng, "Studies of surface coverage and orientation of DNA molecules immobilized onto preformed alkanethiol self-assembled monolayers," *Langmuir*, vol. 16, no. 7, pp. 3272–3280, 2000.

[19] A. W. Peterson, R. J. Heaton, and R. M. Georgiadis, "The effect of surface probe density on DNA hybridization," *Nucleic Acids Research*, vol. 29, no. 24, pp. 5163–5168, 2001.

[20] A. W. Peterson, L. K. Wolf, and R. M. Georgiadis, "Hybridization of mismatched or partially matched DNA at surfaces," *Journal of the American Chemical Society*, vol. 124, no. 49, pp. 14601–14607, 2002.

[21] K. A. Peterlinz, R. M. Georgiadis, T. M. Herne, and M. J. Tarlov, "Observation of hybridization and dehybridization of thiol-tethered DNA using two-color surface plasmon resonance spectroscopy," *Journal of the American Chemical Society*, vol. 119, no. 14, pp. 3401–3402, 1997.

[22] A. B. Steel, R. L. Levicky, T. M. Herne, and M. J. Tarlov, "Immobilization of nucleic acids at solid surfaces: effect of oligonucleotide length on layer assembly," *Biophysical Journal*, vol. 79, no. 2, pp. 975–981, 2000.

[23] T. M. Herne and M. J. Tarlov, "Characterization of DNA probes immobilized on gold surfaces," *Journal of the American Chemical Society*, vol. 119, no. 38, pp. 8916–8920, 1997.

[24] D. V. Leff, L. Brandt, and J. R. Heath, "Synthesis and characterization of hydrophobic, organically-soluble gold nanocrystals functionalized with primary amines," *Langmuir*, vol. 12, no. 20, pp. 4723–4730, 1996.

[25] L. M. Demers, C. A. Mirkin, R. C. Mucic, et al., "A fluorescence-based method for determining the surface coverage and hybridization efficiency of thiol-capped oligonucleotides bound to gold thin films and nanoparticles," *Analytical Chemistry*, vol. 72, no. 22, pp. 5535–5541, 2000.

[26] P. Sandström, M. Boncheva, and B. Åkerman, "Nonspecific and thiol-specific binding of DNA to gold nanoparticles," *Langmuir*, vol. 19, no. 18, pp. 7537–7543, 2003.

[27] W. J. Parak, T. Pellegrino, C. M. Micheel, D. Gerion, S. C. Williams, and A. Paul Alivisatos, "Conformation of oligonucleotides attached to gold nanocrystals probed by gel electrophoresis," *Nano Letters*, vol. 3, no. 1, pp. 33–36, 2003.

[28] S. Park, K. A. Brown, and K. Hamad-Schifferli, "Changes in oligonucleotide conformation on nanoparticle surfaces by modification with mercaptohexanol," *Nano Letters*, vol. 4, no. 10, pp. 1925–1929, 2004.

[29] K. Hamad-Schifferli, J. J. Schwartz, A. T. Santos, S. Zhang, and J. M. Jacobson, "Remote electronic control of DNA hybridization through inductive coupling to an attached metal nanocrystal antenna," *Nature*, vol. 415, no. 6868, pp. 152–155, 2002.

[30] J. J. Storhoff, R. Elghanian, C. A. Mirkin, and R. L. Letsinger, "Sequence-dependent stability of DNA-modified gold nanoparticles," *Langmuir*, vol. 18, no. 17, pp. 6666–6670, 2002.

[31] R. A. Sperling, T. Liedl, S. Duhr, et al., "Size determination of (Bio)conjugated water-soluble colloidal nanoparticles: a comparison of different techniques," *Journal of Physical Chemistry C*, vol. 111, no. 31, pp. 11552–11559, 2007.

[32] T. Pons, H. Tetsuo Uyeda, I. L. Medintz, and H. Mattoussi, "Hydrodynamic dimensions, electrophoretic mobility, and stability of hydrophilic quantum dots," *Journal of Physical Chemistry B*, vol. 110, no. 41, pp. 20308–20316, 2006.

[33] M. Hanauer, S. Pierrat, I. Zins, A. Lotz, and C. Sönnichsen, "Separation of nanoparticles by gel electrophoresis according to size and shape," *Nano Letters*, vol. 7, no. 9, pp. 2881–2885, 2007.

[34] K. A. Ferguson, "Starch-gel electrophoresis—application to the classification of pituitary proteins and polypeptides," *Metabolism*, vol. 13, pp. 985–1002, 1964.

[35] E. Dulkeith, M. Ringler, T. A. Klar, J. Feldmann, A. Muñoz Javier, and W. J. Parak, "Gold nanoparticles quench fluorescence by phase induced radiative rate suppression," *Nano Letters*, vol. 5, no. 4, pp. 585–589, 2005.

[36] D. Zanchet, C. M. Micheel, W. J. Parak, D. Gerion, S. C. Williams, and A. Paul Alivisatos, "Electrophoretic and structural studies of DNA-directed Au nanoparticle groupings," *Journal of Physical Chemistry B*, vol. 106, no. 45, pp. 11758–11763, 2002.

[37] P. Sandström and B. Åkerman, "Electrophoretic properties of DNA-modified colloidal gold nanoparticles," *Langmuir*, vol. 20, no. 10, pp. 4182–4186, 2004.

[38] M.-E. Aubin, D. G. Morales, and K. Hamad-Schifferli, "Labeling ribonuclease S with a 3 nm Au nanoparticle by two-step assembly," *Nano Letters*, vol. 5, no. 3, pp. 519–522, 2005.

[39] W. J. Parak, D. Gerion, D. Zanchet, et al., "Conjugation of DNA to silanized colloidal semiconductor nanocrystalline quantum dots," *Chemistry of Materials*, vol. 14, no. 5, pp. 2113–2119, 2002.

[40] D. Tietz and A. Chrambach, "Analysis of convex ferguson plots in agarose gel electrophoresis by empirical computer modeling," *Electrophoresis*, vol. 7, pp. 241–250, 1986.

[41] D. Tietz and A. Chrambach, "Concave ferguson plots of DNA fragments and convex ferguson plots of bacteriophages: evaluation of molecular and fiber properties, using desktop computers," *Electrophoresis*, vol. 13, no. 1, pp. 286–294, 1992.

[42] B. Tinland, A. Pluen, J. Sturm, and G. Weill, "Persistence length of single-stranded DNA," *Macromolecules*, vol. 30, no. 19, pp. 5763–5765, 1997.

[43] C. Rivetti, M. Guthold, and C. Bustamante, "Scanning force microscopy of DNA deposited onto mica: equilibration versus kinetic trapping studied by statistical polymer chain analysis," *Journal of Molecular Biology*, vol. 264, no. 5, pp. 919–932, 1996.

[44] G. Han, C. T. Martin, and V. M. Rotello, "Stability of gold nanoparticle-bound DNA toward biological, physical, and chemical agents," *Chemical Biology & Drug Design*, vol. 67, no. 1, pp. 78–82, 2006.

[45] M. Cárdenas, J. Barauskas, K. Schillén, J. L. Brennan, M. Brust, and T. Nylander, "Thiol-specific and nonspecific interactions between DNA and gold nanoparticles," *Langmuir*, vol. 22, no. 7, pp. 3294–3299, 2006.

[46] C. K. Kim, R. R. Kalluru, J. P. Singh, et al., "Gold-nanoparticle-based miniaturized laser-induced fluorescence probe for specific DNA hybridization detection: studies on size-dependent optical properties," *Nanotechnology*, vol. 17, no. 13, pp. 3085–3093, 2006.

[47] E. Dulkeith, A. C. Morteani, T. Niedereichholz, et al., "Fluorescence quenching of dye molecules near gold nanoparticles: radiative and nonradiative effects," *Physical Review Letters*, vol. 89, no. 20, Article ID 203002, 4 pages, 2002.

[48] W. J. Qin and L. Y. L. Yung, "Efficient manipulation of nanoparticle-bound DNA via restriction endonuclease," *Biomacromolecules*, vol. 7, no. 11, pp. 3047–3051, 2006.

[49] R. A. Sperling, T. Pellegrino, J. K. Li, W. H. Chang, and W. J. Parak, "Electrophoretic separation of nanoparticles with a discrete number of functional groups," *Advanced Functional Materials*, vol. 16, no. 7, pp. 943–948, 2006.

[50] J. Sharma, R. Chhabra, Y. Liu, Y. Ke, and H. Yan, "DNA-templated self-assembly of two-dimensional and periodical gold nanoparticle arrays," *Angewandte Chemie International Edition*, vol. 45, no. 5, pp. 730–735, 2006.

[51] J. Zheng, P. E. Constantinou, C. Micheel, A. Paul Alivisatos, R. A. Kiehl, and N. C. Seeman, "Two-dimensional nanoparticle arrays show the organizational power of robust DNA motifs," *Nano Letters*, vol. 6, no. 7, pp. 1502–1504, 2006.